Hard gluon damping in hot QCD

André Peshier*

Institut für Theoretische Physik, Universität Giessen, 35392 Giessen, Germany

The gluon collisional width in hot QCD plasmas is discussed with emphasis on temperatures near T_c, where the coupling is large. Considering its effect on the entropy, which is known from lattice calculations, it is argued that the width, which in the perturbative limit is given by $\gamma \sim g^2 \ln(1/g)T$, should be sizeable at intermediate temperatures but has to be small close to T_c. Implications of these results for several phenomenologically relevant quantities, such as the energy loss of hard jets, are pointed out.

I. INTRODUCTION

The dispersion relation and the damping rate of single-particle excitations in many-particle systems are closely related to a variety of phenomenologically important quantities. In a QCD plasma at temperatures much higher than the transition temperature $T_c \sim 200$ MeV, where the coupling g is small and perturbation theory should be applicable, the quark and gluon excitation energies follow directly from the real part of the 1-loop self-energies, which are of the order $(gT)^2$. The calculation of their width, however, requires already to lowest order in g a summation of infinitely many diagrams. Resumming hard thermal loops (HTL), Braaten and Pisarski [1] obtained the widths of quarks and gluons at rest, which are proportional to $g^2 T$. The case of excitations with a finite momentum is more intricate because even with the HTL resummation the result diverges due to the exchange of soft magnetic gluons. With a cutoff of the order of $g^2 T$, either a magnetic mass and/or the width itself, the width of moving charged excitations becomes $\sim g^2 \ln(1/g)T$ on rather general grounds [2]. The logarithm indicates that even in the case of weak coupling the gluon width tests directly the nonperturbative sector of QCD.

A similar breakdown of perturbation theory occurs also in the calculation of the thermodynamic potential $\Omega(T) = -p(T)V$, at order $\mathcal{O}(g^6)$ [3]. The expansion in g, which is known up to $\mathcal{O}(g^6 \ln g^{-1})$ [4], is not reliable (in the sense of systematically improvable with the order) in the physically interesting regime probed in present relativistic heavy ion experiments. For the large coupling strength expected at temperatures near T_c, it does not converge but shows a behavior typical of asymptotic series. In fact, one can hardly expect a converging expansion since it has to be defined in a circle in the complex plane, while in QCD a transition $g^2 \rightarrow -g^2$ is presumably non-analytic. In perturbation theory, this manifests itself in the number of diagrams increasing rapidly with the order. A strategy to remedy the situation in practical calculations is a partial resummation of the perturbative series, taking into account those classes of diagrams whose number increase most rapidly. These are related to the leading orders in the loop expansion in the Φ-derivable approximation scheme [5] to be utilized below. In this scheme, the thermo-dynamic potential is expressed in terms of *dressed* propagators, which are determined self-consistently. The restriction to the leading loop order(s) for large coupling may seem counter-intuitive at first glance. Since it is essential for the following, it is worth mentioning another, yet related, motivation: An asymptotic series, to give the best approximation possible, should be truncated at an order related *inversely* to the coupling; for the QCD thermodynamic potential near T_c possibly already at the order $\mathcal{O}(g^2)$ [6]. Unless the coupling is small, such a low-order perturbative result is, however, not thermodynamically consistent since various thermodynamic quantities are connected to each other by derivatives with respect to the temperature. Since T is also the relevant scale in the running coupling, the derivatives introduce higher orders of the coupling, which for large coupling are not negligible. Therefore, in addition to the leading order(s) in g, a thermodynamically consistent approximation has to resum *some* contributions of higher orders.[1]

A truncation of a resummation scheme based on 2-point functions is, *a priori*, delicate for QCD because of gauge invariance. This problem can be evaded by receding to approximately self-consistent resummations of the thermodynamic potential using appropriate gauge-invariant approximations of the propagators. Indeed, results calculated with HTL propagators [8,9] agree with QCD lattice data down to temperatures of about $3T_c$.[2] The HTL propagators may be reduced even further by neglecting the Landau-damping parts and retaining only the dominant pole contributions, approximating as well the dispersion relations by the asymptotic mass shells. The resulting phenomenological models [11] can describe the lattice data even close to T_c because they allow for an infrared enhancement of the running coupling compared to the 2-loop formula used in [8,9].[3]

---

[1] For a systematic study of resummation improvements of perturbative results, see [7].

[2] Note that the HTL propagators, while derived for soft momenta, have the correct limit for the thermodynamically relevant large momenta near the light cone. The results obtained within 2-loop HTL perturbation theory [10], on the other hand, agree with the lattice data to a lesser extent.

[3] With an infrared-enhanced coupling, also an approximately self-consistent HTL resummation [12] can describe the lattice data down to T_c.

---

*Electronic address: Andre.Peshier@theo.physik.uni-giessen.de

In all of these approaches the observed decrease in the effective degrees of freedom near T_c is directly related to the temperature dependent mass scale $m \sim gT$ that characterizes the excitations. Interpreted as quasiparticles, they become heavy near T_c due to the running coupling and are, thus, suppressed.[4] While this apparently grasps important interaction effects (as motivated above), so far none of the approaches takes into consideration the expected width of the quasiparticles. This, however, is *a priori* not justified for large coupling, when the width might become comparable to the mass of the quasiparticles [14].

In principle, the dressed propagators and the widths can be calculated, by Schwinger-Dyson equations, in the Φ-derivable approximation scheme. However, apart from the aforementioned sensitivity of the width to the soft QCD sector, there is the requirement of gauge invariance of physical quantities such as the width itself or the deduced thermodynamic potential. Moreover, the resummed propagators need to be renormalized nonperturbatively. Notwithstanding the recent progress in these issues [15–17], the problem is involved.

It therefore seems interesting to ask a reversed (and simpler) question: What can be inferred about (important features of) the propagators from quantities which can be reliably calculated by other means? E.g., the thermodynamic bulk properties which are known rather precisely from lattice QCD should, by phase space, reflect relevant properties of the hard excitations with momenta $k \sim T$. Indeed, the large asymptotic masses of the excitations "predicted" in [8,9,11,12] compare nicely with direct results from lattice QCD [18]. To address the width as another characteristic feature I will consider its effect on the entropy, $s = -\partial\Omega/\partial T$. Since s is a measure of the population of phase space, one expects an increased entropy for a system of off-shell particles as described by the width. From the parametric estimate $\gamma \sim g^2 \ln(1/g)T$, the width should become larger with increasing g. This leads to the question whether a large width could be reconcilable with the small entropy near T_c, as calculated on the lattice.

In this paper, some general relations between propagators and entropy will be discussed to approach this question. Section II starts with a brief outline of the formalism of self-consistent approximations, which allows to express the entropy as a simple functional of the propagator. In Sec. III, the case of particles with a Lorentz spectral function is considered in some detail, followed by an analysis of the sensitivity of the results on the spectral function. For the sake of simplicity a scalar field theory is discussed before switching over to QCD in Sec. IV. Given the remarkably universal scaling behavior of the QCD entropy for various numbers of quark flavors [19], I consider here the representative case of the quenched limit of QCD. In the conclusions, some implications of the present findings are pointed out. Some formal details were deferred to the Appendix.

---

[4]For another quasiparticle model see [13].

II. PROPAGATOR AND THERMODYNAMICS

Following the work of Luttinger and Ward [20], the thermodynamic potential Ω of a system of particles with a given interaction can be expressed in terms of the exact 2-point function(s). Considering a scalar theory with the propagator Δ, the expression reads in the imaginary-time formalism (setting the volume $V=1$)

$$\Omega = \frac{1}{2}\sum\kern-1.2em\int (\ln(-\Delta^{-1}) + \Pi\Delta) - \Phi[\Delta], \qquad (1)$$

where $\Pi = \Delta_0^{-1} - \Delta^{-1}$. The contribution $\Phi[\Delta]$ is the sum of the 2-particle irreducible skeleton diagrams; for a $(\kappa/3!)\phi^3 + (g^2/4!)\phi^4$ interaction, it reads

$$\Phi = 3\;\ominus\; + 3\;\infty\; + 12\;\ominus\!\ominus\; + \dots$$

The functional in Eq. (1) is to be evaluated with the exact propagator Δ, which is obtained from the stationarity condition $\delta\Omega[\Delta]/\delta\Delta = 0$. This functional variation is equivalent to

$$\Pi = 2\frac{\delta\Phi}{\delta\Delta}, \qquad (2)$$

i.e., the full self-energy Π is obtained by cutting a full propagator line in the skeleton diagrams of Φ. From this exact representation of Ω, self-consistent ("Φ-derivable") approximations [5] follow by truncation of the expansion of Φ (and, accordingly, the expansion of Π) at a given loop order.

To derive the entropy in terms of the resummed propagator, the Matsubara-sum in Eq. (1) is first transformed into a contour integral in the complex energy plane. After wrapping the contour around the real axis one obtains

$$\Omega = \int_{k^4} n(\omega)\text{Im}(\ln(-\Delta^{-1}) + \Pi\Delta) - \Phi, \qquad (3)$$

where Δ now denotes the retarded propagator; $\int_{k^4} = \int_{k^3}\int d\omega/(2\pi)$, $\int_{k^3} = \int d^3k/(2\pi)^3$, and $n(\omega) = (\exp(\omega/T) - 1)^{-1}$ is the Bose-Einstein distribution function. Taking $\delta\Omega/\delta\Delta = 0$ into account leads to

$$s = -\frac{\partial\Omega}{\partial T} = -\int_{k^4}\frac{\partial n}{\partial T}\text{Im}(\ln(-\Delta^{-1}) + \Pi\Delta) + \frac{\partial\Phi}{\partial T}\bigg|_\Delta$$
$$= s^{dqp} + s', \qquad (4)$$

where

$$s^{dqp} = -\int_{k^4}\frac{\partial n}{\partial T}(\text{Im}\ln(-\Delta^{-1}) + \text{Im}\,\Pi\,\text{Re}\,\Delta), \qquad (5)$$

and

$$s' = -\int_{k^4}\frac{\partial n}{\partial T}\text{Re}\,\Pi\,\text{Im}\,\Delta + \frac{\partial\Phi}{\partial T}\bigg|_\Delta. \qquad (6)$$

Remarkably, the first term in s' exactly cancels the contributions from Φ with one and two vertices. This cancellation is basically a topological feature and holds also in other theories [21], including QCD [8]. This implies that the contribution (5), given the propagator, is the leading-loop resummed entropy in the Φ-derivable scheme, which in the context of Fermi liquid theory is sometimes called the *dynamical quasiparticle contribution* to the entropy. According to the arguments put forward in the Introduction, it is a preferable approximation of the exact entropy at large coupling,[5]

$$s \simeq s^{dqp} = s^{(0)} + \Delta s. \tag{7}$$

Although this approximation is genuinely nonperturbative, it has a simple 1-loop structure and it does not depend on the vertices. For the decomposition in Eq. (7), the integrand in Eq. (5) is rewritten using

$$\mathrm{Im}\,\ln(-\Delta^{-1}) = \pi\,\mathrm{sgn}(\mathrm{Im}\,\Delta) - \arg(\Delta)$$

$$= \pi\,\mathrm{sgn}(\mathrm{Im}\,\Delta)\Theta(\mathrm{Re}\,\Delta)$$

$$- \arctan(\mathrm{Im}\,\Delta/\mathrm{Re}\,\Delta).$$

In the first term, the real part of the propagator is negative for small $\omega > 0$, as shown below, and it changes sign at $\omega^2 = \omega_k^2$. Using $\mathrm{sgn}(\mathrm{Im}\,\Delta(\omega)) = -\,\mathrm{sgn}(\omega)$, this term yields the expression of the entropy of free bosons with the dispersion relation ω_k (and zero width),

$$s^{(0)} = \frac{1}{T}\int_{k^3}(-T\ln(1 - e^{-\omega_k/T}) + \omega_k n(\omega_k)). \tag{8}$$

In the following, ω_k will simply be referred to as the "dispersion relation" of the dynamical quasiparticles although it need not to coincide with the real part of the pole (if existent) of the propagator. The effects of a non-zero spectral width are solely due to the remaining contributions,

$$\Delta s = \int_{k^4}\frac{dn}{dT}\left(\arctan\lambda - \frac{\lambda}{1 + \lambda^2}\right), \tag{9}$$

where $\lambda = \mathrm{Im}\,\Delta/\mathrm{Re}\,\Delta$. For later reference it is noted that the second term in the parenthesis is $\mathrm{Im}\,\Delta$ times the derivative of the phase $\arctan\lambda$ with respect to $\mathrm{Im}\,\Delta$.

The sum of the expressions (8) and (9) yields the dynamical quasiparticle entropy as an approximation of the exact entropy (for notational convenience the differentiation will be omitted in the following) as a functional of the propagator. Facing the mentioned difficulties in the calculation of the

---

[5]With regard to the application in QCD it is emphasized that the cancellation in s' holds for any propagator, in particular for the exact one. Parametrizing later the exact gluon propagator by the dispersion relation and the width, which are physical quantities, ensures the gauge invariance of the results. At the same time, reasoning along the same lines as in the Introduction, the deviation of the entropy calculated from the self-consistent and from the exact propagator should be small.
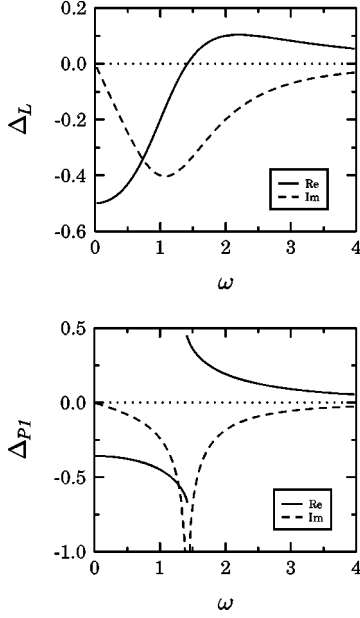
dressed propagator, the entropy functional will be evaluated with various physically motivated *Ansätze* for the propagator, taking into account the width. Verified first, under rather general assumptions, is the expectation that the entropy is increased for a non-zero spectral width, $\Delta s > 0$. To this end, the analytic propagator, for complex k_0, is expressed in the Lehmann representation,

$$\Delta^a(k_0, \mathbf{k}) = \int_{-\infty}^{\infty}\frac{d\omega}{2\pi}\frac{\rho(\omega, \mathbf{k})}{k_0 - \omega}. \tag{10}$$

The spectral function is the discontinuity of the propagator at the real axis,

$$\rho(\omega, \mathbf{k}) = \Delta^a(\omega - i\epsilon, \mathbf{k}) - \Delta^a(\omega + i\epsilon, \mathbf{k}), \tag{11}$$

which is real, odd in ω with $\omega\rho(\omega) \geq 0$, and it satisfies the sum rule

$$\int_{-\infty}^{\infty}\frac{d\omega}{2\pi}\omega\rho(\omega, \mathbf{k}) = 1 \tag{12}$$

for all values of $\mathbf{k}$. This implies that the propagator approaches the free limit at large k_0,

$$\Delta^a(k_0, \mathbf{k}) = \int_0^{\infty}\frac{d\omega}{\pi}\omega\frac{\rho(\omega, \mathbf{k})}{k_0^2 - \omega^2} \overset{k_0 \to \infty}{\longrightarrow} \frac{1}{k_0^2}.$$

These general properties of the spectral function have several implications for the retarded propagator $\Delta(\omega) = \Delta^a(\omega + i\epsilon)$. Its imaginary part, which by the reflection principle is $-\frac{1}{2}\rho(\omega)$, satisfies

$$\mathrm{Im}\,\Delta(\omega = 0) = 0,$$

$$\mathrm{Im}\,\Delta \leq 0 \quad \text{for } \omega > 0,$$

$$\mathrm{Im}\,\Delta \to 0 \quad \text{for } \omega \to \infty.$$

Similarly, one readily infers

$$\mathrm{Re}\,\Delta(\omega = 0) = -\int\frac{d\omega'}{2\pi}\frac{\rho(\omega')}{\omega'} < 0,$$

$$\mathrm{Re}\,\Delta \to \omega^{-2} \quad \text{for } \omega \to \infty,$$

and that odd-order derivatives of $\mathrm{Re}\,\Delta(\omega)$ vanish at $\omega = 0$. Now consider a generic spectral function with a dominant peak near ω_k and a characteristic width γ, and possibly with some additional minor substructures. In this case $\mathrm{Re}\,\Delta(\omega)$ changes its sign only once for $\omega > 0$, i.e., the "dispersion relation" ω_k is unique, which will be the only assumption for the following argument. In principle then, there are two typical cases of propagators, see Fig. 1: (i) the imaginary part is regular, and the real part is smooth, and (ii) the imaginary part is singular [but integrable due to Eq. (12)], and the real part is discontinuous. Common to both cases is that the dispersion relation ω_k of the dynamical quasiparticles is determined by the real part of the self-energy,

FIG. 1. The real and the imaginary parts of the propagators Δ_L and Δ_{P1} defined in Eq. (16) and in Sec. III E, respectively. All quantities are in units of the width γ, and the energy scale E in the spectral functions is chosen such that $\omega_k = \sqrt{2}$.

$$\mathrm{Re}\,\Delta^{-1}(\omega_k) = \Delta_0^{-1}(\omega_k) - \mathrm{Re}\,\Pi(\omega_k) = 0. \tag{13}$$

The dispersion relation ω_k and the peak position in ρ coincide for singular spectral functions, but not necessarily for regular spectral functions. The integrand of the entropy contribution Δs is discontinuous at ω_k; shown in Fig. 2 is the parenthesis term in Eq. (9). This factor is, in an approximate
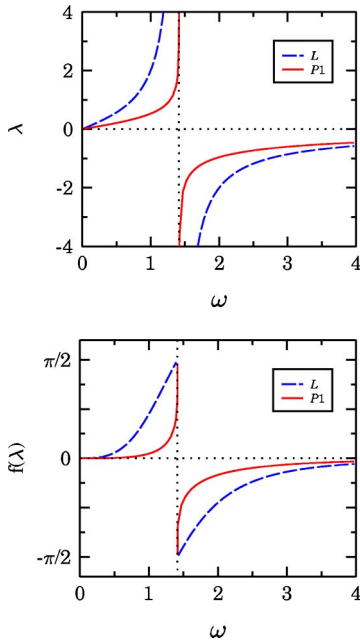

FIG. 2. The functions $\lambda = \mathrm{Im}\,\Delta / \mathrm{Re}\,\Delta$, and $f(\lambda) = \arctan\lambda - \lambda/(1+\lambda^2)$ [occurring in Eq. (9) in the integrand of Δs] for the propagators shown in Fig. 1.

way, symmetric near ω_k, where $\lambda(\omega) = \mathrm{Im}\,\Delta / \mathrm{Re}\,\Delta$ is singular. Since the second factor in the integrand in Eq. (9),

$$\frac{dn}{dT} = \frac{\omega}{T^2} \frac{\exp(\omega/T)}{(\exp(\omega/T) - 1)^2}, \tag{14}$$

is monotonically decreasing with ω, it is plausible that $\Delta s > 0$. A rigorous argument is given in the Appendix. From Fig. 2 it can also be expected that the entropy increase is smaller for singular spectral functions than for regular ones.

III. SPECTRAL FUNCTIONS

A. Lorentz spectral function

In the previous section, the spectral function was introduced to deduce some general properties of the propagator and the entropy. At the same time it is more intuitive (and more efficient due to the analytic properties) to model the spectral function rather than the propagator. From the spectral function of free relativistic particles with $\Delta_0^{-1} = k_0^2 - \omega_m^2$, where $\omega_m^2 = m^2 + \boldsymbol{k}^2$,

$$\rho_0(\omega) = 2\pi[\delta((\omega - \omega_m)^2) - \delta((\omega + \omega_m)^2)],$$

an often used *Ansatz* to describe non-zero width is obtained by replacing the δ-function by a Lorentzian,

$$\rho_L(\omega) = \frac{\gamma}{E}\left(\frac{1}{(\omega - E)^2 + \gamma^2} - \frac{1}{(\omega + E)^2 + \gamma^2}\right). \tag{15}$$

The corresponding retarded propagator can be easily calculated by a contour integration,

$$\Delta_L(\omega) = \frac{1}{\omega^2 - E^2 - \gamma^2 + 2i\gamma\omega}.$$

In general, the analytical continuation of the retarded propagator to complex energies is analytic in the upper plane. In the present case it has poles in the lower plane, at $k_0 = \pm E - i\gamma$. The parameter E is also related to the dispersion relation (13) of the dynamical quasiparticles. Choosing $E^2(\boldsymbol{k}) = \boldsymbol{k}^2 + m^2 - \gamma^2$,[6] the propagator becomes

$$\Delta_L(\omega, \boldsymbol{k}) = \frac{1}{\omega^2 - \boldsymbol{k}^2 - m^2 + 2i\gamma\omega}. \tag{16}$$

With this convention, the parameter m^2 corresponds directly to the real part of the retarded self-energy. This has the advantage that the dispersion relation does not depend on γ, $\omega_k = \omega_m$.

---

[6]There is no ambiguity in the spectral function (15) for $\gamma^2 > \boldsymbol{k}^2 + m^2$ as obvious from the alternative representation $\rho_L = 4\gamma\omega/(\omega^2 - E^2 - \gamma^2)^2 + 4\gamma^2\omega^2)$. Note, however, that the spectral function becomes slightly more asymmetric, and that the poles of the propagator (16), at $k_0 = -i\gamma \pm (\omega_m^2 - \gamma^2)^{1/2}$, turn purely imaginary for $\gamma > \omega_m$.
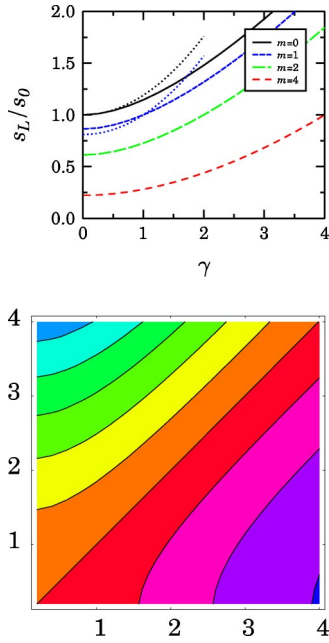
FIG. 3. Top: The entropy $s_L(m, \gamma)$ as a function of γ for several values of m (γ and m are in units of T). The dotted lines show the expansion (19) for $m=0$ and $m/T=1$. Bottom: Contour plot of s_L/s_0; the contour spacing is 0.25, and the straight line marks $s(m, \gamma) = s_0$.

Turning now to the entropy, one should note that in general the mass and the width parameters are momentum-dependent. The resulting effects will be considered below; for now the parameters are assumed to be constant. For the propagator (16), the contribution (8) to the dynamical quasi-particle entropy,

$$s_L^{(0)}(m) = \frac{1}{T} \int_{k^3} (-T \ln(1 - e^{-\omega_m/T}) + \omega_m n(\omega_m/T)),$$

$$(17)$$

is simply the entropy of free bosons with mass m. Corresponding expressions for QCD have been the starting point in the approaches [11], which interpreted the thermodynamically relevant transverse gluon and the quark particle-excitations as quasiparticles with masses given by the asymptotic self-energies (and respective degeneracies). The contribution (9) due to the non-zero width reads explicitly

$$\Delta s_L(m, \gamma) = \int_{k^4} \frac{\partial n}{\partial T} \left(\arctan \frac{2\gamma\omega}{\omega_m^2 - \omega^2} \right.$$

$$\left. - 2\gamma\omega \frac{\omega_m^2 - \omega^2}{(\omega^2 - \omega_m^2)^2 + (2\gamma\omega)^2} \right). \quad (18)$$

A numerical integration shows—in line with the general expectation—that the total entropy $s_L = s_L^{(0)} + \Delta s_L$ increases with the width and decreases with m, cf. Fig. 3. An notable detail is that $s_L(m = \gamma)$ is equal to the Stefan-Boltzmann entropy of the massless ideal gas, $s_0 = \frac{4}{90}\pi^2 T^3$. This is proven in the Appendix, where also the expansion
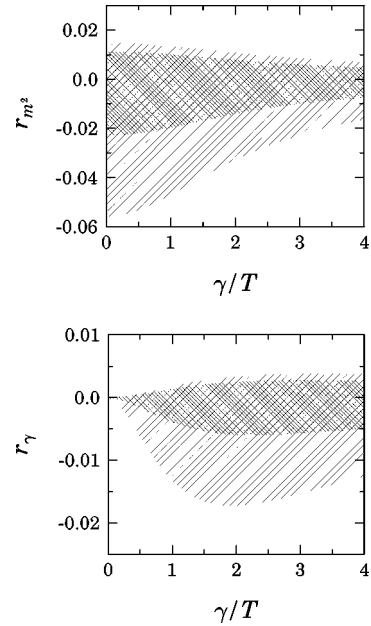

FIG. 4. The sensitivity (20) of the entropy s_L on the momentum dependence of m^2 (top) and γ (bottom). The parameters are varied for $k < T$ (see text) in the range $[\frac{1}{4}, 4]$ (outer band) and $[\frac{1}{2}, 2]$ (inner band). In both cases the asymptotic mass is $m = 4T$.

$$s_L(m, \gamma) = s_0 \left[1 - \frac{15}{8\pi^2} \frac{m^2}{T^2} + \frac{15}{8\pi^2} \frac{\gamma^2}{T^2} + \cdots \right] \quad (19)$$

for small values of m and γ is derived. It is interesting to note that this result coincides with the expansion of the contribution $s_L^{(0)}$ with complex masses, $s_L(m, \gamma) \approx \frac{1}{2}(s_L^{(0)}(m + i\gamma) + s_L^{(0)}(m - i\gamma))$.

B. Momentum-dependent mass and width parameters

Due to phase space, thermodynamic bulk properties are determined by hard momenta. Therefore, the entropy is expected to be not very sensitive on the exact momentum dependence of the width as well as on the dispersion relation (described by a momentum dependent mass parameter) at soft momenta. To quantify this expectation, the squared mass and the width are varied for $k < T$ by some factor from m^2 and γ, which are now considered as the asymptotic values. Denoting the resulting entropy by $\tilde{s}_L$, the quantity

$$r = 1 - \frac{\tilde{s}_L}{s_L}, \quad (20)$$

provides a measure of the momentum sensitivity. As shown in Fig. 4, r is indeed only of the order of a few percent when varying the dispersion relation.

The sensitivity to the low-momentum behavior of the width is even less. The figures show the sensitivity for a rather large asymptotic mass; for smaller masses the sensitivity is even lower. This quantifies the expectation that the entropy is, to the extent required below, insensitive to details of the propagator at soft momenta.
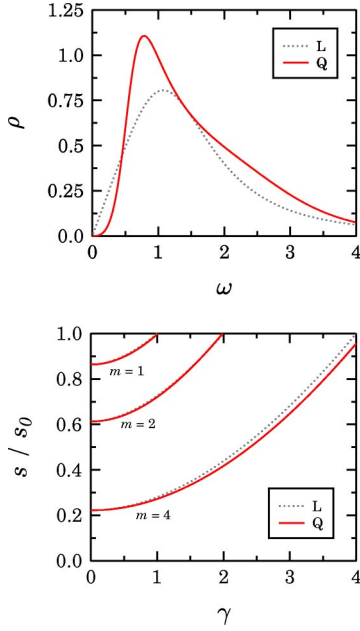
FIG. 5. Top: The spectral functions of the propagators Δ_L and Δ_Q with $\omega_m = \sqrt{2}$ (all quantities are in units of γ); if $\gamma = T$, this corresponds, e.g., to $k = m = T$. Bottom: The corresponding entropies as functions of γ and m (in units of T); for small masses the lines practically coincide.

C. Specific shape of spectral function

For a first test of the sensitivity to the specific form of the spectral function, let us consider the normalized function

$$\rho_Q(\omega) = \frac{\sqrt{2}\,\gamma^3}{E}\left(\frac{1}{(\omega - E)^4 + \gamma^4} - \frac{1}{(\omega + E)^4 + \gamma^4}\right),$$

which has a more pronounced peak than the Lorentzian (15). It can be expressed in terms of the function ρ_L with complex width parameters,

$$\rho_Q[\gamma] = \frac{1}{\sqrt{2}}(\sqrt{i}\rho_L[\sqrt{i}\,\gamma] + \sqrt{-i}\rho_L[\sqrt{-i}\,\gamma]). \quad (21)$$

An analogous relation easily allows to obtain the corresponding propagator in terms of the Lorentz propagator (16). Replacing furthermore $\gamma \to \sqrt{2}\,\gamma$, the result reads

$$\Delta_Q(\omega, \boldsymbol{k}) = \frac{a^3 + 2ab^2 - 4ib^3}{a^4 + 4b^4}, \quad (22)$$

where $a = \omega^2 - \omega_m^2$ and $b = 2\gamma\omega$. The propagator (22) coincides with $\Delta_L(\omega, \boldsymbol{k})$ for $\omega \to 0$ and $\omega \to \pm\infty$ as well as on the common mass shell $\omega^2 = \omega_m^2$. Thus, differences in the entropies can indeed be attributed to the spectral form rather than to a change in the dispersion relation.

The differences in the propagators Δ_L and Δ_Q, apart from the analytic structure, are considerable for typical values of the 4-momentum; see Fig. 5. Nonetheless, there is almost no effect on the entropy even for large values of m and γ. This example leads to the question which features of ρ the en-

tropy is actually sensitive to. Already expected in Sec. II were differences between the two generic types of spectral functions shown in Fig. 1. In any case, the integrand of the contribution (9) is notably different from zero only for energies $|\omega - \omega_k| \lesssim \gamma$, cf. Fig. 2. A way to focus on this relevant interval is to consider large times, $t > \gamma^{-1}$, in the Fourier transform $\rho(t)$ of the spectral function.

D. Spectral functions in Fourier space

The Fourier transform of the spectral function is defined by

$$\rho(t) = \int_{-\infty}^{\infty} \frac{d\omega}{2\pi} e^{-i\omega t} \rho(\omega). \quad (23)$$

The sum rule (12),

$$1 = \int_{-\infty}^{\infty} \frac{d\omega}{2\pi} \omega\rho(\omega) = \int_{-\infty}^{\infty} dt\,\rho(t) \int_{-\infty}^{\infty} \frac{d\omega}{2\pi} \omega e^{i\omega t},$$

which after a partial integration becomes $i\int dt\,\dot{\rho}(t)\delta(t)$, translates into

$$\left.\frac{d\rho(t)}{dt}\right|_{t=0} = -i. \quad (24)$$

It is plausible that the sum rule tests the short-time behavior in Fourier space since in momentum space it is closely related to the fact that the propagator approaches the free limit at large energies. The Lorentzian spectral function (15), with

$$\rho_L(t) = \exp(-\gamma|t|)\frac{\sin Et}{iE},$$

obviously complies with the condition (24). From the fact that the oscillations and the attenuation of $\rho(t)$ are related to the position and the width, respectively, of the peak of $\rho(\omega)$, one can easily construct other conceivable spectral functions. In the *Ansatz*

$$\rho_f(t) = f(t)\frac{\sin Et}{iE}, \quad (25)$$

functions with $f(0) = 1$ provide candidates for possible spectral functions if $\omega\rho(\omega) \geq 0$ is satisfied.

The similar entropies for the propagators Δ_L and Δ_Q, shown in Fig. 5, may now be attributed to the similar long-time behavior of the spectral functions [with the replacement $\gamma \to \sqrt{2}\,\gamma$, which led to the propagator (22), also $\rho_Q(t)$ decreases as $\exp(-\gamma t)$, cf. Eq. (21)]. Before studying this in more detail, it is noted that in terms of $\rho(t)$ the retarded propagator reads

$$\Delta(k_0) = i^{-1}\int_0^{\infty} dt\,e^{ik_0 t}\ \rho(t). \quad (26)$$

For the *Ansatz* (25),

TABLE I. Damping models for $\rho(t)$, cf. Eq. (25), together with their Fourier transforms $\mathcal{F}$ as defined in Eq. (28). $\Gamma(0,z)$ denotes the incomplete Γ-function, K_0 is the modified Bessel function of the second kind, L_0 is the modified Struve function, Erf is the error function, and $x = \omega/\gamma$.

Model	$f(t)$	$\gamma \mathcal{F}(\omega)$
L	$\exp(-\gamma\lvert t\rvert)$	$(1-ix)^{-1}$
P_1	$(1+\gamma\lvert t\rvert)^{-1}$	$e^{-ix}\Gamma(0,-ix)$
P_2	$(1+\gamma\lvert t\rvert)^{-2}$	$1+ixe^{-ix}\Gamma(0,-ix)$
$\vdots$	$\vdots$	$\vdots$
P_n	$(1+\gamma\lvert t\rvert)^{-n}$	$(1+ix[\gamma\mathcal{F}_{n-1}])/(n-1)$
$P_1^\star$	$(1+(\gamma t)^2)^{-1/2}$	$K_0(\lvert x\rvert)+\dfrac{\pi}{2}\mathrm{sgn}(x)[I_0(\lvert x\rvert)-L_0(\lvert x\rvert)]$
G	$\exp(-(\gamma t)^2)$	$\frac{1}{2}\sqrt{\pi}\exp(-(x/2)^2)[1+\mathrm{Erf}(ix/2)]$

$$\Delta_f(k_0) = \frac{i}{2E}\int_0^\infty dt\, e^{ik_0 t}(e^{iEt} - e^{-iEt})f(t)$$

$$= \frac{i}{2E}(\mathcal{F}(k_0+E) - \mathcal{F}(k_0-E)), \qquad (27)$$

the propagator can be expressed by a "retarded" Fourier transform of the function $f(t)$,

$$\mathcal{F}(\omega) = \int_0^\infty dt\, e^{i\omega t} f(t). \qquad (28)$$

E. Non-exponential time behavior

Although often assumed, an exponential decrease of $\rho(t)$ is not dictated by any fundamental requirement [22]. In any case, as already argued, the contribution (9) to the entropy due to the nonzero width is determined by the long-time behavior of the spectral function; it will increase if $\rho(t)$ decreases faster, either by a larger value of γ or due to the functional form of $\rho(t)$. In the following, this is demonstrated systematically by some models for the spectral function (25), which are summarized in Table I.

In the models P_1 and $P_1^\star$, $\rho(t)\sim f(t)$ decreases asymptotically as t^{-1}. This implies that the spectral function

$$\rho(\omega) = -2\,\mathrm{Im}\,\Delta(\omega) = -\frac{1}{E}(\mathcal{F}_c(\omega+E) - \mathcal{F}_c(\omega-E)),$$
$$(29)$$

where $\mathcal{F}_c(\omega) = \int_0^\infty dt\,\cos\omega t f(t)$ is the cosine transform of $f(t)$, diverges logarithmically at $\omega = \pm E$, see Figs. 1 and 6. For $\gamma\to 0$, the free propagator is recovered. For the model P_1, e.g., this follows from $\Gamma(0,x) = e^x(x^{-1}+\cdots)$ for $x\to\infty$. Moreover, the incomplete Γ-function $\Gamma(0,z)$ is discontinuous at the negative axis. Accordingly, the retarded propagator Δ_{P1} has cuts in the lower k_0-plane, starting at the singularities. The entropies for the models P_1 and $P_1^\star$ are shown in Fig. 6.

As anticipated before, the entropy increases with γ much less than in the case of a regular spectral function. On the
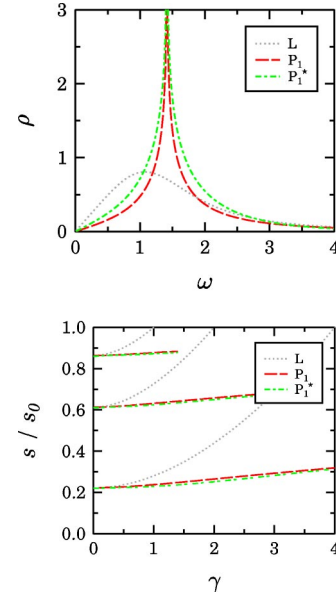

FIG. 6. Comparison of the models P_1 and $P_1^\star$ with L, analogous to Fig. 5. The entropies almost coincide for the cases P_1 and $P_1^\star$.

other hand, the deviations between the models P_1 and $P_1^\star$ are only at the level of a few percent. This quantifies that the entropy is indeed sensitive to the long-time behavior of $\rho(t)$, while the short-time behavior is far less relevant.

In the models P_n, the spectral function decreases as t^{-n}. Since for different n the functions $f_{P_n}(t)$ are related by derivatives with respect to t, their Fourier transform (28) can be calculated by a simple recursion relation given in Table I. Figure 7 shows the spectral functions for $n = 1\ldots 4$ along
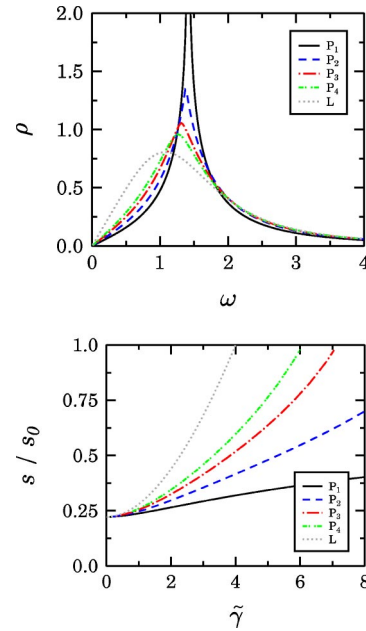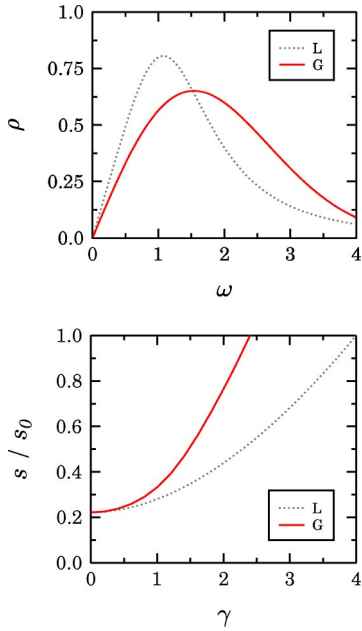

FIG. 7. Results for the models $P_n (n = 1\ldots 4)$, similar to Fig. 5. The upper plot compares the spectral functions ρ_n with a width parameter $\gamma_n = \tilde{\gamma}/n$ and ρ_L with $\gamma = \tilde{\gamma} = 1$; the lower plot shows the entropies as a function of $\tilde{\gamma}$.

FIG. 8. Results for the Gaussian model G, analogous to Fig. 5.

with the corresponding entropies. Plotting s as a function of $\tilde{\gamma}=n\gamma$ confirms again the general expectation that the entropy is not determined by the short-time behavior $\rho_n(t) \approx 1 - \tilde{\gamma}t$, but rather by the large-time behavior of the spectral function. As expected, the faster $\rho(t)$ decreases, the larger the entropy. Leaving the class of polynomial models, this trend is also obvious when considering the Gaussian model G in Fig. 8.

To conclude this section, the entropy functional (7) is, in general, sensitive to the spectral width of the hard modes. Numerically, the effects of the width and that of a mass shift are comparable, also if both are large, $m \sim \gamma \sim T$. Details are closely related to the long-time behavior of the Fourier transform of the spectral function.

IV. QCD

In QCD, the entropy for various numbers of quark flavors, plotted as a function of T/T_c and scaled by the free limit, has a remarkably universal behavior as found in lattice calculations [19]. I focus here on the representative case of the quenched limit of QCD, and point out briefly expected differences for the physical case.

The gluon propagator has a transverse and a longitudinal part which leads to a corresponding decomposition of the entropy. In the Φ-derivable approach, the contributions have the form (5) multiplied by the respective degeneracies [8]. The longitudinal modes are collective excitations whose spectral strength is exponentially suppressed for larger momenta, which leads to only a minor contribution to the entropy. In the perturbative limit, it is of the order g^3 while the transverse modes yield a $\mathcal{O}(g^2)$ term. Also for larger coupling the longitudinal contribution is rather small as demon-

strated in the HTL calculations [8,9].[7] Taking therefore into account only the dominating transverse excitations with the propagator Δ, the resummed entropy reads

$$s = -2(N_c^2 - 1) \int_{k^4} \frac{\partial n}{\partial T} (\operatorname{Im} \ln(-\Delta^{-1}) + \operatorname{Im} \Pi \operatorname{Re} \Delta).$$

(30)

In a self-consistent approximation, the propagator will have a residual gauge dependence, leading to an unphysical result for the entropy. However, as motivated before, a parametrization of the exact propagator by the dispersion relation and the width, which are gauge-invariant, can be used in Eq. (30).

The *Ansatz* of the quasiparticle models [11] is to neglect the width altogether, and to describe the propagator simply by the perturbative self-energy on the light-cone, which is a gauge-invariant mass term,[8]

$$M^2 = \frac{N_c}{6} g^2 T^2,$$

(31)

where $N_c = 3$. The resulting ''minimal'' resummation of the entropy can indeed nicely describe the lattice data for all temperatures above T_c if an infrared enhancement of the running coupling is permitted, for example in the form [11]

$$g^2(T) = \frac{48\pi^2}{11 N_c \ln(\lambda(T-T_s)/T_c)^2}.$$

(32)

For the physical number of degrees of freedom, $d_g = 2(N_c^2 - 1)$, a fit of the parameters λ and T_s/T_c leads in the entropy to small but systematic deviations from the lattice result for $T > 2T_c$, cf. fit 1 in Fig. 9. This can be improved when considering d_g as an additional parameter in fit 2, which yields a value not too far from the physical one, cf. Table II.[9]

Taking now into account the width on the same footing as the mass (31), I will first consider a perturbative *Ansatz* for γ. In the weak coupling limit, the width of a hard transverse gluon was obtained by Pisarski [23] in a resummed calculation,

---

[7]This approach might actually overestimate the longitudinal contribution since at very large g it leads to a negative result for the total entropy. This is due to the negative definite ghost contribution which in Ref. [8] is implicitly included in the longitudinal contribution.

[8]Being the only scale in the HTL propagators, the asymptotic mass (31) appears also in the calculations [8,9].

[9]While in the first reference [11] finite-size effects of the lattice data or the contribution of the longitudinal modes were considered as possible explanations, the latter does not seem likely after the net longitudinal contribution was found to be negative in the HTL calculation [8].
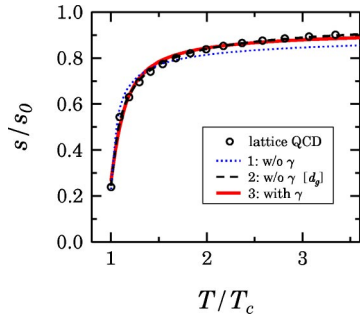
FIG. 9. The entropy of the SU(3) plasma in units of the free entropy. The symbols represent the lattice data [24]. Fits without width are depicted by the dotted and dashed line, for the latter d_g was also fitted (see text). The full line is the fit 3 with the width. The parameters are summarized in Table II.

TABLE II. The parameters of the fits shown in Fig. 9.

	λ	T_s/T_c	d_g	c
fit 1	10.5	0.88	16 (fixed)	-
fit 2	5.2	0.76	17.5	-
fit 3	2.6	0.50	16 (fixed)	14.0

$$\gamma = \frac{N_c}{8\pi} g^2 T \left(\ln \frac{\frac{2}{3} M^2}{m_{\text{mag}}^2 + 2 m_{\text{mag}} \gamma} + 1.09681 \ldots \right). \quad (33)$$

Several assumptions have been made here: (i) soft gluons are HTL dressed while intermediate hard gluons have a Lorentzian spectral function; (ii) the divergence from the static magnetic gluons is screened assuming that this sector of QCD can be parametrized by a mass $m_{\text{mag}} \sim g^2 T$. The first supposition follows the concept of a self-consistent calculation, hence γ appears also on the right hand side of Eq. (33) as a regulator next to the magnetic mass. Since the argument of the logarithm is basically g^{-2}, the width of moving excitations is parametrically enhanced compared to the width at rest, $\gamma(0) \sim g^2 T$. Implicit with (i) is the supposition of a simple pole structure of the propagator, which, however, is not warranted by any fundamental requirement. In fact, the result (33) could only be justified, to separate the pole from a branching point, if $\gamma \ll m_{\text{mag}}$ (although the converse relation was considered more likely). While the constraint was necessary to explore details of the cut-off, the generic behavior $\gamma \sim g^2 \ln(1/g) T$ is expected on general grounds [2]. Therefore, and to keep the connection to the result (33), I analyze the SU(3) entropy with the Lorentz spectral function and the width in the form[10]

$$\gamma = \frac{3}{4\pi} \frac{M^2}{T^2} T \ln \frac{c}{(M/T)^2}, \quad (34)$$

where c parametrizes the soft cut-off. It is emphasized that because the functional relation between M and γ is fixed, it is not obvious whether a fit of the entropy lattice data is possible at all, or that introducing c in addition to the param-

eters in the coupling (32) will improve the result of the fits 1 and 2. The numerics shows, however, that this is indeed the case. The enhanced entropy, due to the width, nicely explains the small deviations of fit 1 for $T \gtrsim 2$ without having to adjust d_g as in fit 2. As to be expected, the mass is somewhat larger than in the previous fits, cf. Fig. 10.

More interesting is the behavior of the width near T_c. Because there s/s_0 is small, the mass and hence the coupling have to be large. At the same time, the width cannot be too large since it would over-compensate the decreasing effect of the mass. Within the *Ansatz* (34) this implies that the logarithm has to become small. It is worth to emphasize that the optimal value of c, given in Table II, is surprisingly close to the value

$$c^\star = \frac{M^2(T_c)}{T_c^2} \approx 13.7, \quad (35)$$

so the width vanishes almost precisely at T_c (and is indeed positive for all temperatures).[11] Interestingly then, the condition $\gamma \ll m_{\text{mag}}$, which was necessary in the derivation of Eq. (33) (but originally considered to not represent the physical situation), can actually be fulfilled in a small vicinity of T_c. Taking the next-to-leading logarithm result at face value leads to an estimate of the magnetic mass which is consistent below $1.1 T_c$, where $m_{\text{mag}} > 2\gamma$. This estimate (including the "predicted" range of applicability) is indeed in nice agreement with the lattice data [25] as shown in Fig. 11. The magnetic mass at T_c, which is difficult to calculate on the lattice, is estimated as

$$m_{\text{mag}}(T_c) \approx \sqrt{\frac{2}{c}} \frac{M(T_c)^2}{T_c} \approx 5 T_c. \quad (36)$$

For larger temperatures, the behavior of the magnetic mass follows the form $m_{\text{mag}} = d g^2 T$. Note that the fit from Ref. [25], which uses the 2-loop running coupling at the momentum scale $2\pi T$, can be improved by using the coupling as obtained in fit 3.

It is emphasized that the magnetic and the electric screening masses have a qualitatively different large-coupling behavior: The electric screening mass, as known from lattice calculations [25], becomes *small* near T_c. This is readily understood in the quasiparticle model [11], where

---

[10]I mention that although Pisarski considered massless hard gluons, his result also holds true for *small* masses $\sim gT$ due to a cancellation in the energy difference of the inner and outer gluon. Note also that the resummation of a width $\sim g^2 \ln(1/g) T$ can generate powers of logs in the expansion of thermodynamic quantities, cf. Eq. (19).

[11]It is noted that although the parameter c is closely related to the small entropy at T_c, it also tests the global behavior of $s(T)$.
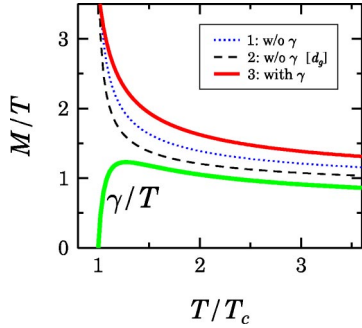
FIG. 10. The masses and the width according to the fits shown in Fig. 9.

$$m_{\mathrm{D}}^2 = \Pi_{00}(\omega=0, \boldsymbol{p}\to 0) = -2g^2 N_c \int_{k^3} \frac{\partial n}{\partial \omega}\bigg|_{\omega_m}. \tag{37}$$

Near T_c, the excitations are narrow (thus the quasiparticle picture is justified) and heavy, and the Debye mass

$$m_{\mathrm{D}}^2 \sim g^2 \ g^{3/2} e^{-M/T} \ T^2 \tag{38}$$

is Boltzmann-suppressed. It is noted that the decrease of the Debye mass cannot be expected, even tendentiously, from the next-to-leading order perturbative result [26],[12]

$$m_{\mathrm{D,n}}^2 = m_{\mathrm{D,0}}^2 \left[1 + \frac{\sqrt{3 N_c}}{2\pi} g \left(\ln \frac{2 m_{\mathrm{D,n}}}{m_{\mathrm{mag}}} - \frac{1}{2} \right) \right]. \tag{39}$$

Coming back to the discussion of the width, it is plausible from the properties of the entropy [e.g., from the fact $s_L(m = \gamma) = s_0$ mentioned in Sec. III] that the width has to be rather small near T_c. However, the functional form (34), even as an extrapolation of the perturbative form similar to Eq. (31), is *a priori* not justified near T_c where M becomes large (see footnote 10). Physically, one would rather expect a Boltzmann suppression of the heavy thermal fluctuations, leading to

$$\bar{\gamma} = A e^{-bg} g^\nu \ T. \tag{40}$$

For lack of better knowledge, I take this generic form as an *Ansatz* for large coupling, and smoothly connect it to the "perturbative" form (34) with the adjusted values of $\{\lambda, T_s/T_c, c\}$, by

$$\gamma^\star = (1-\Theta) \bar{\gamma} + \Theta \gamma, \tag{41}$$

with $\Theta(T) = \frac{1}{2} + \pi^{-1} \arctan((T-\bar{T})/\delta)$. Since the fit function s/s_0 can basically be described by 3 parameters (say by the values at T_c and in the saturation-like regime, and by the slope at T_c), a conclusive determination of the parameters

---

[12]Although apart from the more obvious solution, which is larger than the leading-order result $m_{\mathrm{D,0}} = (N_c/3)^{1/2} g T$, there is a second smaller solution [at T_c, with Eq. (36), $\bar{m}_{\mathrm{D,n}} \approx 0.4 m_{\mathrm{D,0}}$], the latter is unphysical because it does not connect to the perturbative result for $g \to 0$.
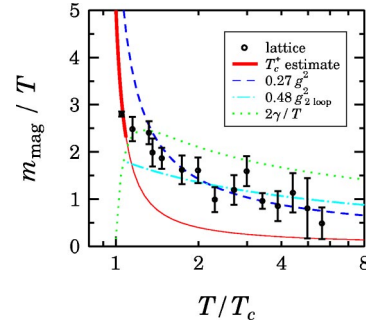

FIG. 11. The lattice data [25] for the magnetic gluon mass, and the estimate based on Eq. (33) with the fitted width, which is meaningful only in a small vicinity of T_c, i.e., only for the left data point (see text). Also shown are the $g^2 T$-fits with the 2-loop running coupling [25] (dash-dotted line) and, respectively, with the adjusted coupling (32) from fit 3 (dashed line).

$\{A, b, \nu, \bar{T}, \delta\}$ cannot be expected. In any case, within the enlarged parameter space the improvements in χ^2 compared to fit 3 are only of the order of a few percent. The changes in the plot of the mass and the width, including the distinguished behavior at T_c, are almost invisible. This robustness of the results justifies *a posteriori* the usage of the perturbative *Ansatz* (34) also for smaller temperatures.

For larger T, after a distinguished maximum at

$$T_\gamma \approx 1.3 T_c, \tag{42}$$

the ratio γ/T decreases very slowly. Different from what the parametric form of Eq. (34) might suggest, the width is even for very large T to a good accuracy proportional to the mass; for T/T_c in [5,100],

$$\frac{\gamma}{M} \approx 0.69 - 0.02 \ln \frac{T}{T_c}. \tag{43}$$

This underlines the fact that in this range of temperatures quasiparticle models as [8,9,11,12] can provide "only" an effective description, while a relation of the quasiparticles to the actual excitations may be difficult. Near T_c, on the other hand, the transverse hard excitations may be directly interpreted as quasiparticles (with some additional substructure due to Landau-damping etc.) as visualized in Fig. 12. This concept is beneficial since (up to rather large temperatures) the coupling is large: terms of higher order in g contribute significantly in the resummed entropy.

For definiteness, I have considered here the case of a Lorentz spectral function. However, from the results of Sec. III E it is obvious that the main result—a small width near T_c—should hold true also for other spectral functions, unless their Fourier transform has an exotic long-time behavior such as $\rho(t) \sim t^{-1}$, which is not to be expected.

V. CONCLUSIONS

In this work it was shown for the deconfined SU(3) plasma that the collisional width (or damping rate) of hard gluons should be sizeable at intermediate temperatures, but
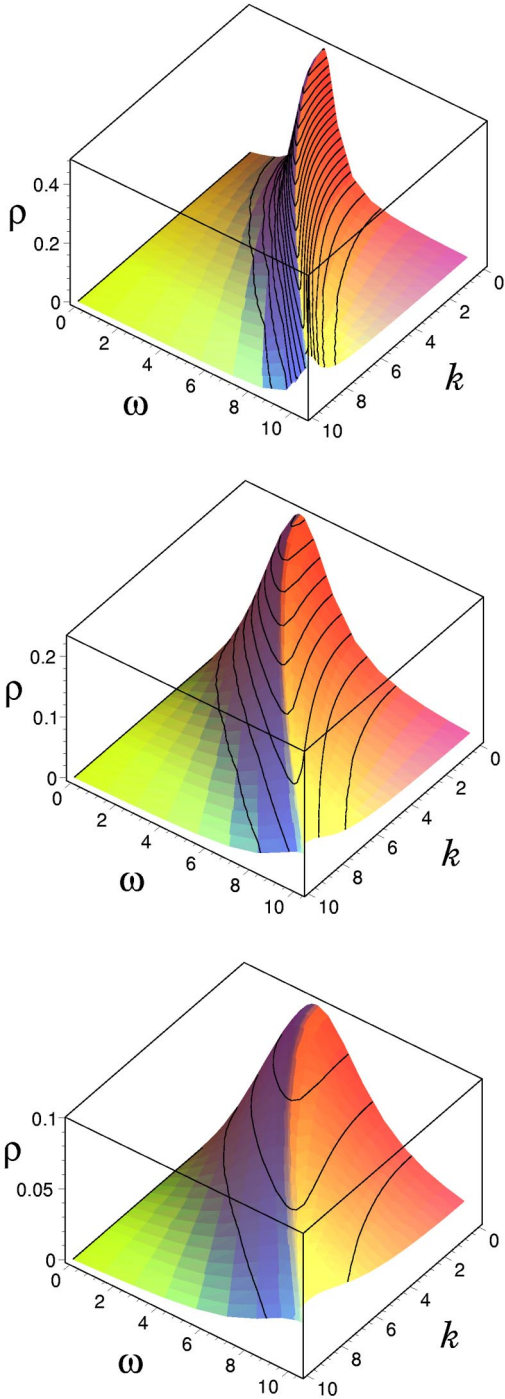
FIG. 13. The lattice data [25] for the gluon Debye mass vs the rescaled width from fit 3.

FIG. 12. The Lorentzian gluon spectral function from fit 3 for $T/T_c = 1.03$, 1.35, 3 (ω, k and ρ are in units of T). Shown here is the full phase space although the present approach can make statements only for hard momenta of the order of T.

has to become small near T_c. While from an extrapolation of the parametric estimate $\gamma \sim g^2 \ln(1/g) T$ (with the logarithm read as an enhancement factor) this result may seem surprising, a large width would be hard to reconcile with the small entropy near T_c as established in lattice calculations. For QCD with dynamical quarks, the rescaled entropy has a similar temperature dependence [19], albeit the lattice data
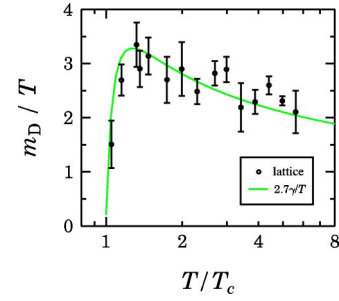
are so far less precise. Therefore, the main result of a reduced width near the transition should carry over from the quenched to the physical case. Although in full QCD the ratio s/s_0 is slightly larger at T_c, which is related to the nature of the transition, and the widths of the hard transverse gluons and quark particle-excitations might not vanish, a quasiparticle picture (in the actual meaning) of the strongly coupled QCD plasma close to T_c may be justified.

There are several interesting implications of the characteristic temperature dependence of the width besides those for the screening properties discussed above. As the inverse of the mean free path λ, the width is closely related to transport properties as, e.g., equilibration times. Expecting a critical slowing-down near a phase transition provides another indication that the width has to become small near T_c. Another quantity, which is of particular interest with regard to the interpretation of SPS and RHIC experiments, is the radiative energy loss of hard quarks and gluons transversing the plasma. The results derived in Ref. [27] for a system of length L under the assumption of (several) independent scatterings, i.e. $m_D \gg \gamma$, which is not unrealistic in the situation of interest (see below), are characterized by the energy scale

$$E_{cr} = \gamma m_D^2 L^2. \tag{44}$$

In the Landau-Pomeranchuk-Migdal regime, for parton energies $E > E_{cr}$, the total energy loss reads [27]

$$-\Delta E = \frac{1}{8} C_R \alpha \gamma m_D^2 L^2 \ln \gamma L, \tag{45}$$

where R indicates the color representation of the parton. As argued in [28], already the expected "critical" behavior of the screening mass m_D would lead to a reduced energy loss at temperatures near T_c, possibly explaining the absence of jet quenching at SPS energies [29]. With the temperature dependence of the width obtained here, the reduction of the energy loss is even more pronounced. Having adjusted the temperature dependence of α and γ to lattice data may allow for realistic estimates. In order to describe also the Debye mass in a simple way, without further assumptions, I make use of the empirical observation that for the relevant temperatures the lattice data [25] are roughly proportional to the width,

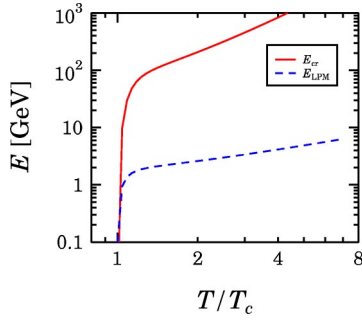$$m_D \approx 2.7 \gamma, \tag{46}$$

FIG. 14. The temperature dependence of the energy scales E_{cr} and E_{LPM} for the radiative energy loss. The length of the medium was set to $L=5$ fm, and $T_c=170$ MeV.

cf. Fig. 13. The resulting behavior of the energy scale E_{cr}, shown in Fig. 14, changes drastically at

$$T_E \approx 1.3 T_c. \tag{47}$$

Close to T_c, the energy E_{cr} becomes very small. Already for slightly larger temperatures it is well above the scale $E_{LPM} = m_D^2/\gamma$ which is relevant for the energy loss in the Bethe-Heitler regime. A similar sudden onset, also around T_E, is found for the total energy loss, cf. Fig. 15. For larger temperatures the estimated energy loss agrees basically with other results, while close to T_c it becomes very small and would be hard to observe experimentally. Similar small results have been obtained for the corresponding SPS energies in Ref. [30].

In summary, it has been argued from the reduced number of degrees of freedom near the transition temperature that the width of hard excitations has to become small near T_c. While for QCD this was demonstrated under the assumption of a Lorentz spectral function, the propagator may have a more complicated pole structure. For hot QED (where no
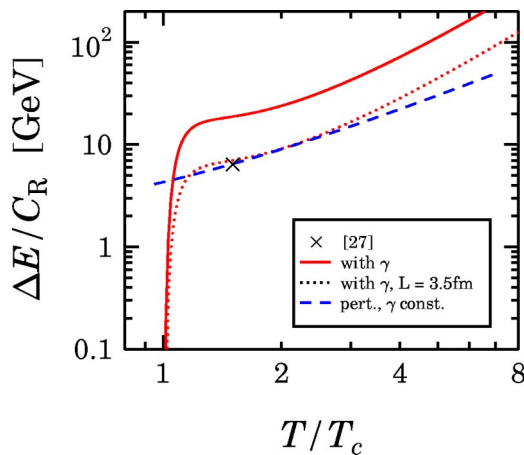

FIG. 15. The radiative energy loss from Eq. (45) for $L=5$ fm, unless indicated otherwise. The symbol is an estimate from Ref. [27]. The dashed line results from a 2-loop running coupling, with m_D set to $m_{D,0}$ and a constant γ to match the result from [27]. The full line is the estimate with the T-dependent width and the adjusted coupling, as is the dotted line where $L=3.5$ fm was assumed to illustrate the scaling behavior.

magnetic mass exists), the fermion propagator has been calculated in a Bloch-Nordsieck approach [31]. The infrared-finite result is an *entire* function of the energy. Nonetheless, the spectral function is strongly peaked, with a characteristic width $\sim e^2 \ln(1/e)T$. Since in Fourier space it decreases faster than an exponential, the effect for the entropy will be even more pronounced than for a Lorentzian spectral function. Although the situation may be different in QCD, a spectral function which has only little effect on the entropy, with $\rho(t) \sim t^{-1}$, seems hard to explain. Therefore, although from the entropy calculated in lattice QCD nothing can be inferred about the analytic structure of the propagator, the general result of small widths near T_c is arguably robust. This implies a characteristic change of several phenomenologically relevant quantities at $T^\star \approx T_\gamma \approx T_E \approx 1.3 T_c$.

APPENDIX: SOME PROPERTIES OF Δs

In the following it is argued that the entropy is generally increased for a non-zero width, i.e. $\Delta s > 0$ in Eq. (9). Furthermore, considering the Lorentz spectral function, the expansion of $s_L(m, \gamma)$ is calculated for small arguments. Finally it is proven that $s_L(m, \gamma)$ is for $m=\gamma$ equal to the Stefan-Boltzmann value $s_0 = s^{(0)}(m=0) = (4\pi^2/90)T^3$.

In order to prove (under the assumption of a unique dispersion relation ω_k) that $\Delta s > 0$, consider the relevant integral in Eq. (9) in the form

$$I = \int_0^\infty d\omega \, \frac{\partial n(\omega)}{\partial T} f(\lambda(\omega)),$$

where $f = \arctan \lambda - \lambda/(1+\lambda^2)$, with $\lambda = \text{Im}\,\Delta/\text{Re}\,\Delta$. Changing the integration variable to λ,

$$I = \int_{-\infty}^\infty d\lambda \, \frac{\partial \omega}{\partial \lambda} \, \frac{\partial n(\omega(\lambda))}{\partial T} f(\lambda),$$

the integrand becomes a product of three factors, of which $f(\lambda)$ is an odd function. The sign of I is, thus, determined only by the other two terms, which can be discussed on the basis of the relation $\omega(\lambda)$, whose inverse is shown in Fig. 2. In particular, $\omega \to \{0, \omega_k-0, \omega_k+0, \infty\}$ corresponds to $\lambda \to \{0^+, +\infty, -\infty, 0^-\}$. Then, via the inverse derivative $\partial\lambda/\partial\omega$ and the properties of the propagator listed in Sec. II, it is easily inferred that $\partial\omega/\partial\lambda$ is positive and that it vanishes for $|\lambda| \to \infty$, is non-zero for $\lambda \to 0^+$, and diverges for $\lambda \to 0^-$, cf. Fig. 16. The product $(\partial\omega/\partial\lambda)(\partial n/\partial T)$, however, vanishes for small negative λ due to the second factor, which for the corresponding large ω is exponentially suppressed. At small positive λ, on the other hand, this factor is Bose enhanced, $\partial n/\partial T \sim \omega^{-1}$, while it approaches the value $\partial n/\partial T|_{\omega_k}$ for $\lambda \to \pm\infty$. Therefore, the integral of
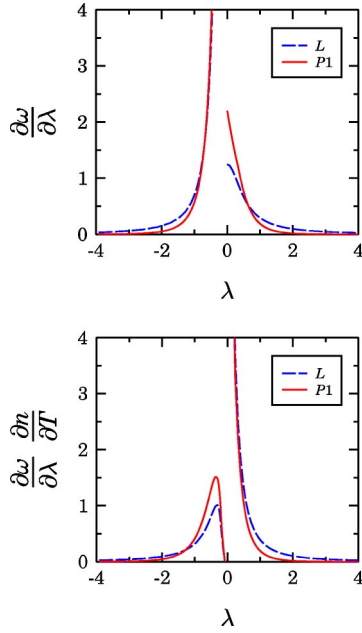
FIG. 16. Two functions used in the argumentation that $\Delta s > 0$, for the case of the propagators from Fig. 1.

$(\partial\omega/\partial\lambda)(\partial n/\partial T)$ over $[-\infty,0]$ is finite, while for the interval $[\varepsilon,+\infty]$ it approaches $+\infty$ for $\varepsilon\to 0$. This shows that the integral I, whose integrand includes the odd function $f(\lambda)$, is positive (and finite due to $f\sim\lambda^3$ for small λ), hence $\Delta s > 0$.

Turning now to the expansion of the entropy $s_L(m,\gamma) = s^{(0)}(m) + \Delta s_L(m,\gamma)$ for a Lorentzian spectral function, I introduce the notation $\Gamma = 2\gamma$ and follow the remark below Eq. (9), writing

$$\Delta s_L(m,\Gamma) = \int_0^\infty \frac{d\omega}{\pi}\frac{\partial n}{\partial T}\int_{k^3}\left(h - \Gamma\frac{\partial h}{\partial\Gamma}\right),$$

where $h = \arctan(\Gamma\omega/(\omega_m^2 - \omega^2))$. Considering first the case $m = 0$, i.e., $\omega_m = k$, the two terms of the k-integrand decrease as k^{-2}. In the subtracted integral

$$\mathcal{I} = \int_{k^3}\left(\frac{\partial h}{\partial\Gamma} - \frac{\omega}{k^2}\right)$$

$$= \frac{\omega}{2\pi^2}\int_0^\infty dk\, k^2\left(\frac{k^2 - \omega^2}{(k^2 - \omega^2)^2 + \Gamma^2\omega^2} - \frac{1}{k^2}\right),$$

the substitutions $k = x\omega$ and $a = \Gamma/\omega$ lead to

$$\mathcal{I} = \frac{\omega^2}{2\pi^2}\int_0^\infty dx\, x^2\left(\frac{x^2 - 1}{(x^2 - 1)^2 + a^2} - \frac{1}{x^2}\right)$$

$$= -\frac{\omega^2}{2\pi^2}\frac{\pi}{2\sqrt{2}}(\sqrt{1 + a^2} - 1)^{1/2} = -\frac{\omega\Gamma}{8\pi} + \cdots.$$

The remaining ω-integral yields

$$\mathcal{J} = \int_0^\infty \frac{d\omega}{\pi}\frac{\partial n}{\partial T}\mathcal{I} = -\frac{T}{24}\Gamma + \cdots.$$

From $\Delta s_L(m,\Gamma) = \int d\Gamma\, \mathcal{J} - \Gamma\mathcal{J}$, and since $\Delta s_L(m,\Gamma = 0) = 0$ (for any m), one obtains

$$\Delta s_L(m = 0,\Gamma) = \frac{T}{48}\Gamma^2 + \cdots.$$

Furthermore, it is obvious that derivatives of any order of $\Delta s_L(m,\Gamma)$ with respect to m vanish at $\Gamma = 0$. Therefore, the leading term in m in the expansion of the total entropy comes entirely from the contribution $s^{(0)}(m)$, which is well known, and one arrives at the expression (19).

Finally, the fact that $s_L(m,\gamma = m) = s_0$ holds not only in the limit of small m and γ is readily proven by verifying $\partial s_L(m,\gamma = m)/\partial m = 0$. After taking the derivative of the integrand of the total entropy,[13] the k-integration yields zero, indeed. As an aside it is mentioned that for $\gamma \geq m$, the poles of the propagator (16) are purely imaginary for some range of momenta, see footnote 6.

---

[13]Note that the integrand of s_L, contrary to the integrand of Δs_L, cf. Eq. (18), is a smooth function of m.

[1] E. Braaten and R.D. Pisarski, Phys. Rev. D **42**, 2156 (1990).

[2] R.D. Pisarski, Phys. Rev. Lett. **63**, 1129 (1989); V.V. Lebedev and A.V. Smilga, Ann. Phys. (N.Y.) **202**, 229 (1990).

[3] A.D. Linde, Phys. Lett. **96B**, 289 (1980).

[4] K. Kajantie, M. Laine, K. Rummukainen, and Y. Schröder, Phys. Rev. D **67**, 105008 (2003).

[5] G. Baym, Phys. Rev. **127**, 1391 (1962).

[6] A. Peshier, J. High Energy Phys. **01**, 040 (2003).

[7] J.P. Blaizot, E. Iancu, and A. Rebhan, Phys. Rev. D **68**, 025011 (2003).

[8] J.P. Blaizot, E. Iancu, and A. Rebhan, Phys. Rev. D **63**, 065003 (2001).

[9] A. Peshier, Phys. Rev. D **63**, 105004 (2001).

[10] J.O. Andersen, E. Braaten, E. Petitgirard, and M. Strickland, Phys. Rev. D **66**, 085016 (2002).

[11] A. Peshier, B. Kämpfer, O.P. Pavlenko, and G. Soff, Phys. Rev.

D **54**, 2399 (1996); P. Levai and U. Heinz, Phys. Rev. C **57**, 1879 (1998); A. Peshier, B. Kämpfer, and G. Soff, *ibid.* **61**, 045203 (2000); Phys. Rev. D **66**, 094003 (2002).

[12] A. Rebhan and P. Romatschke, Phys. Rev. D **68**, 025022 (2003).

[13] R.A. Schneider and W. Weise, Phys. Rev. C **64**, 055201 (2001).

[14] S. Juchem, W. Cassing, and C. Greiner, Phys. Rev. D **69**, 025006 (2004).

[15] A. Arrizabalaga and J. Smit, Phys. Rev. D **66**, 065014 (2002).

[16] H. van Hees and J. Knoll, Phys. Rev. D **65**, 025010 (2002); **65**, 105005 (2002); **66**, 025028 (2002).

[17] J.P. Blaizot, E. Iancu, and U. Reinosa, Nucl. Phys. **A736**, 149 (2004).

[18] P. Petreczky *et al.*, Nucl. Phys. B (Proc. Suppl.) **106**, 513 (2002).

[19] F. Karsch, E. Laermann, and A. Peikert, Phys. Lett. B **478**, 447 (2000).

[20] J.M. Luttinger and J.C. Ward, Phys. Rev. **118**, 1417 (1960).

[21] E. Riedel, Z. Phys. **210**, 403 (1968); G.M. Carneiro and C.J. Pethick, Phys. Rev. B **11**, 1106 (1975); B. Vanderheyden and G. Baym, J. Stat. Phys. **93**, 843 (1998).

[22] A. L. Fetter and J. D. Walecka, *Quantum Theory of Many-Particle Systems* (McGraw-Hill, New York, 1971).

[23] R.D. Pisarski, Phys. Rev. D **47**, 5589 (1993).

[24] M. Okamoto *et al.*, Phys. Rev. D **60**, 094510 (1999).

[25] A. Nakamura, T. Saito, and S. Sakai, Phys. Rev. D **69**, 014506 (2004).

[26] A. Rebhan, Phys. Rev. D **48**, 3967 (1993).

[27] R. Baier, Yu.L. Dokshitzer, A.H. Mueller, S. Peigne, and D. Schiff, Nucl. Phys. **B483**, 291 (1997).

[28] A. Dumitru and R.D. Pisarski, Phys. Lett. B **525**, 95 (2002).

[29] X.N. Wang, Phys. Lett. B **579**, 299 (2004).

[30] M. Gyulassy, P. Levai, and I. Vitev, Phys. Rev. Lett. **85**, 5535 (2000).

[31] J.P. Blaizot and E. Iancu, Phys. Rev. D **55**, 973 (1997).